



LARGE SCALE EXPERIMENTAL INVESTIGATION OF SPECIAL MOMENT RESISTING CONNECTIONS IN STEEL PLATE SHEAR WALLS

R. Purba⁽¹⁾, M. Moestopo⁽²⁾

⁽¹⁾ Assistant Professor, Department of Civil Engineering, Universitas Bandar Lampung (UBL), Indonesia, ronnypurba@ubl.ac.id

⁽²⁾ Associate Professor, Department of Civil Engineering, Institut Teknologi Bandung (ITB), Indonesia, moestopo@si.itb.ac.id

Abstract

Past research in steel plate shear walls (SPSWs) reported that plastic hinge rotation demands at the ends of horizontal boundary elements (HBE) are expected to be large. This high rotation demand would be difficult to achieve using the ordinary-type connections specified in the AISC 2016 Seismic Specifications for HBE connection to vertical boundary elements (VBE). Moreover, fractures of HBE-to-VBE connections at lower drift would prevent SPSW specimen to perform as an effective seismic force resisting system of which normally is specified to achieve a higher target drift. This paper presents the results of a large-scale experimental investigation on the behavior of special moment resisting connections (SMRC) in SPSWs. Two types of the prequalified connections specified in the AISC 358-16 documents were investigated, namely the welded unreinforced flange-welded web (WUF-W) and reduced beam section (RBS). A total of 8 SMRC connections were investigated (4 connections for each type considered). After pushover cyclic tests with target drifts at the top beam gradually increased from 0.06% to 3.0% drift, large flange local buckling, significant plastification, or fractures occurred at all SMRC connections. This research also provided an additional evidence that ordinary-type connections used in SPSWs might not be sufficient to sustain large rotation demand that could develop in those HBE-to-VBE connections.

Keywords: steel plate shear walls; welded unreinforced flange-welded web; reduced beam section; plastic hinge; special moment resisting connection



1. Introduction

Steel plate shear walls (SPSW) that consists of unstiffened infill plate connected to the surrounding boundary frames have been validated as an effective system to resist lateral loads. Compared to other lateral force resisting systems (e.g., moment resisting and braced frames), SPSW could provide significant strength and stiffness to buildings. Consequently, the system has been implemented in many mid- to high-rise buildings as their main earthquake load resisting system [1, 2]. An extensive review on the development, design philosophy, modeling, analytical and experimental studies, and codification of SPSWs can be found in past publications (e.g., [1, 2, 3, 4]).

Past experimental studies reported failures of boundary elements could possible lead to deterioration of SPSWs [5, 6, 7, 8, 9]. Moment resisting connections designed to connect horizontal boundary elements (HBE) to vertical boundary elements (VBE) in several of those SPSWs tested also suffered boundary element failures, after experienced relatively large plastic rotations. The types of failures reported include localized flange and web buckling that lead to plastic hinge development, flange and web fractures at HBE ends, weld fractures, and shear tab failure [10].

Recently, Purba and Bruneau [11] conducted an experimental investigation to assess the performance of special moment resisting connections, namely the welded unreinforced flange-welded web (WUF-W) connection. Several WUF-W connections experienced fractures at HBE ends after suffered large rotation ranges (absolute difference between rotations recorded in the positive and negative excursions) even though absolute rotations in one particular displacement cycle might not be that large. They suggested that the ordinary-type connection specified by the AISC code [3] might not be sufficient to sustain large rotation demand. It is important to note, however, not all AISC 358-10 [12] prescribed limits and details for the WUF-W connections were respected in the 1/3 scaled connections used in that study. To validate those findings and recommendations in [11], this paper presents the results of large-scale pushover cyclic tests on two SPSW specimens designed with the WUF-W and reduced beam section (RBS) type connections between its boundary elements.

2. Design of experimental program

Two SPSW specimens were prepared and tested. Testing was conducted at the Research Institute for Human Settlement (known in Indonesia as the Pusat Penelitian dan Pengembangan Perumahan dan Permukiman (PUSKIM), Ministry of Public Works and Housing). The actuator capacity available at the PUSKIM facility (capable of transferring maximum force and displacement of 1,000 kN and 200 mm, respectively) dictated the dimension of SPSW specimens. In addition, the aforementioned intent to fully comply with the dimensional requirements for the AISC 358-16 prequalified moment connections [13] dictated selection of boundary frame members. As its schematic view shown in Fig. 1(a), the specimens have equal height and width dimensions of 2500 mm, measured between boundary frame member centerlines. Note that the resulting geometry of the SPSW specimens is approximately half-scale of that could be used in typical steel structures.

Capacity design principles were used to design the specimens. Here, story forces (forces from the actuator) were resisted entirely by the infill plate without considering the strength contribution provided by the surrounding boundary frames, the boundary frames then resisted tension forces generated by an assumed fully yielding condition of the infill plate, and in-span plastic hinges were explicitly prevented to occur along the boundary frames [7, 14]. When maximize the actuator capacity, per Eq. F5-1 of the AISC 2016 Seismic Provisions [15], low yield strength (LYS) steel of 1.3 mm thick was selected for the specimen infill plate. Sizing the boundary frames per procedures by [7] and [16], WF400×200×8×12 and WF350×175×7×11 were selected for the columns and beams, respectively. The names of Indonesian designation wide-flange (WF) I-shapes reflect their depth, flange width, as well as web and flange thicknesses. The average material properties from a total of 5 tensile coupons of each component are summarized in Table 1. Two pre-qualified



special moment resisting connections specified in the AISC 358-16 documents [13] were considered. The WUF-W type connection was designed for all four HBE-to-VBE connections in the first SPSW specimen (WUF-W Specimen), while that in the second specimen, the RBS type connection was used (RBS Specimen). Detail dimensions of RBS is shown in Fig. 1(c).

Table 1 – Summary of Material Properties from Tensile Coupon Test

Component	Yield Strength (MPa)	Ultimate Strength (MPa)	Rupture Strain (%)
Column	340	455	22
Beam	340	455	22
Infill Plate	40	128	20

3. Experimental setting

Fig. 1(b) shows a photograph of experimental setup in the PUSKIM facility. The specimen was positioned in the East to West direction, supported by two hinges at the base of columns similar to that in [7], fastened to a 650×650×50 mm base plate using eight 19 mm diameter bolts on each column, and then anchored to the 1 m thick concrete strong floor using 4 high strength tension rods at each column. The clevis hinge center point was 530 mm from the centerline of the bottom beam.

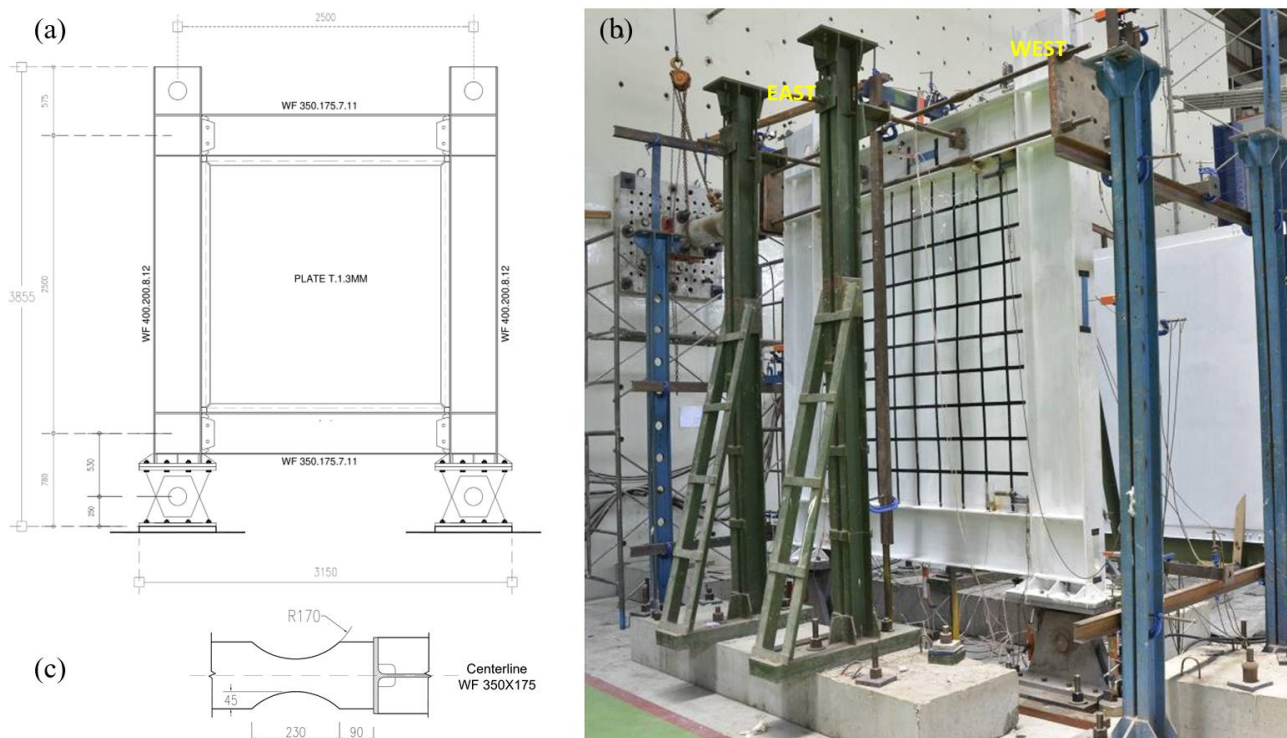


Fig. 1 – SPSW Specimen: (a) Elevation View; (b) Experimental Setup; (c) RBS Detail

An existing “belt” consists of four high strength tension rods and a connecting plate at each end of the rods was utilized for each experimental program. When the rods fastened, the belt clamped the specimen at the level of top beam to simulate simultaneous lateral displacement between East and West columns as in the case of a rigid floor. One static hydraulic actuator was then attached to the East connecting plate to laterally load the specimen. Two existing framings on each side of the specimen were used to provide lateral supports to the specimen with rollers touched the top beam at two locations, as shown in Fig. 1(b).



3.1 Instrumentation

The specimens were instrumented to collect experimental data, including displacement transducers, uniaxial strain gauges, load cell, and video cameras. The applied load was obtained directly from the load cell attached to the actuator. Infill plate behavior was measured qualitatively by means of visible gridlines spaced at 210 mm horizontally and vertically on both sides of the infill plate. This allowed for observations of plate buckling and yielding (indicated by flaking of whitewash).

Fig. 2(a) shows instrumentation layout for the displacement transducers. The transducers provided various measurements including lateral displacements at the centerline of the top and bottom beams as well as at the mid-high of the left and right columns, panel zone deformations, beam-to-column joint rotations, out-of-plane displacement, and uplifts at the pin supports. Instrumentation layout for uniaxial strain gauges is shown in Fig. 2(b). A group of four strain gauges measured strains at expected plastic hinge locations, 205 mm from the face of columns.

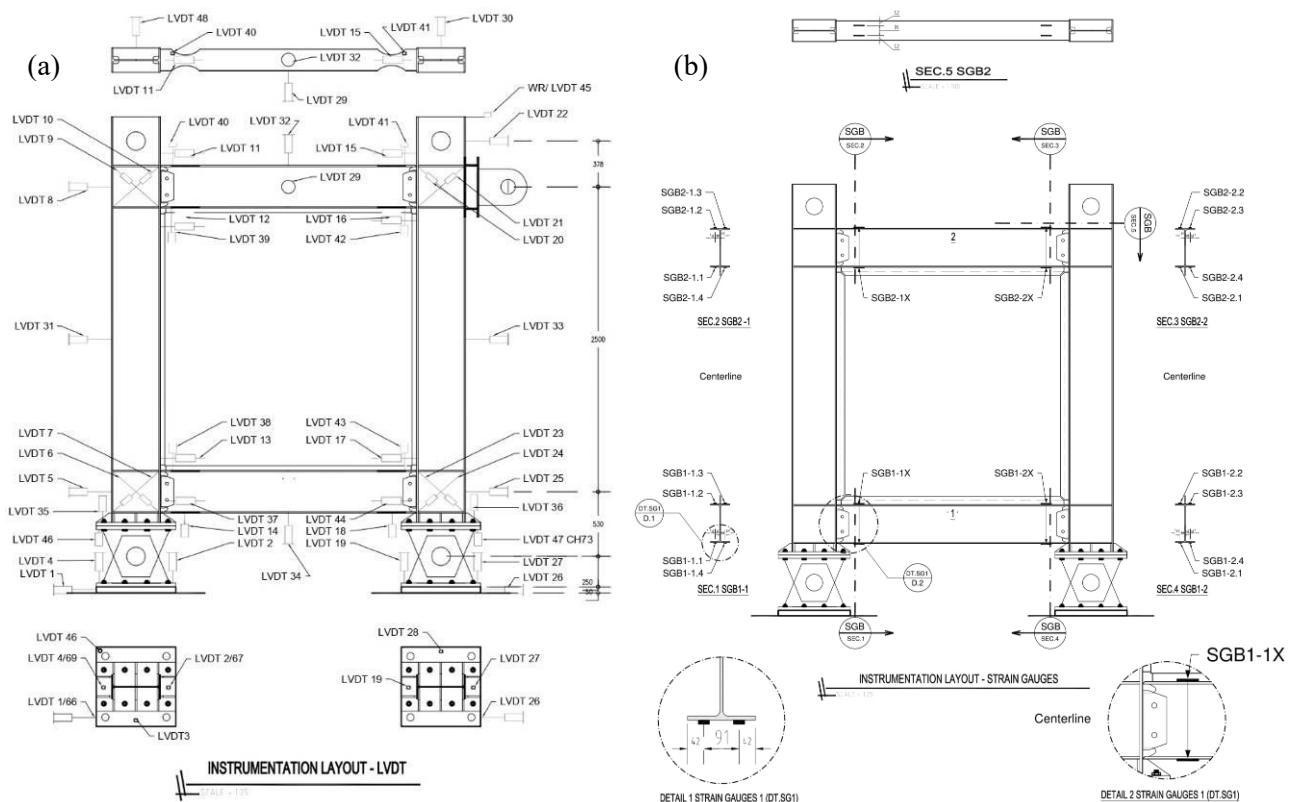


Fig. 2 – Instrumentation Layout: (a) Displacement Transducers; (b) Uniaxial Strain Gauges

3.2 Loading Protocol

Similar to that in [7, 11], the loading protocol for these experimental programs started with the loading sequences specified in the ATC-24 protocol [17] that are formulated as a function of ductility ratio (μ) and followed afterward the AISC Seismic Provisions [13] requirements that are in terms of drift. Here, the ductility ratio is defined as the ratio of the specimen lateral displacement (Δ) to the specimen effective yield displacement (δ_y). The latter was determined as the point where the elastic and inelastic tangents intersected to each other on a force-displacement pushover curve of one specimen analytical model in SAP2000, using material coupon testing data (Table 1). The resulting δ_y were 12.4 and 12.0 mm, corresponding to a drift of 0.36% and 0.35% for the WUF-W and RBS specimens, respectively.

The tests were carried out in a displacement-control quasi-static cyclic loading. The initial three displacement steps were $1/6$, $1/3$, and $2/3$ of the estimated effective yield displacement. The specimens were



cycled three times for each displacement step. After this point, the maximum target displacements were increased by multiples of δ_y until reaching an estimated ductility of three. Afterward, the target displacements continued to increase by an estimated ductility of four, but the number of cycles was decreased to two cycles. Beyond this point, the target amplitudes were increased by drift increments until reaching 2.5% and 3.0%, consecutively. Fig. 3 shows a typical loading protocol for these experimental programs, with a total of 9 displacement steps and a cumulative 24 cycles to be applied to the specimen.

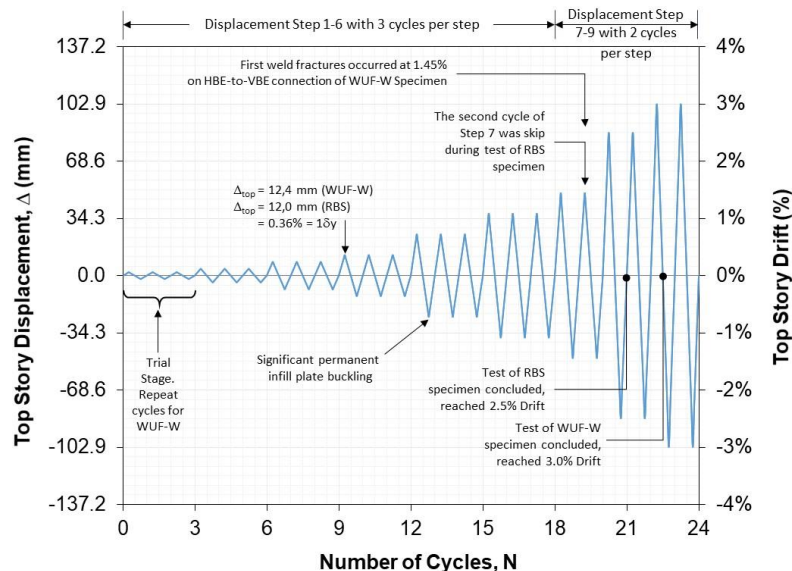


Fig. 3 – Cyclic Displacement Loading History

4. Experimental observations and results

4.1 WUF-W Specimen

The experiment began with three trial cycles at 2.1 mm target displacement (corresponding to 0.06% top story drift or $\frac{1}{6}\delta_y$) to observe whether all experimental setting working as planned. With minor fixes on the instrumentation, the test continued with repeated cycles of the same target displacement, and then followed by a target maximum displacement gradually increased from 2.1 mm to 12.4 mm (from 0.06% to 0.36% drift or ductility ratio increased from $\frac{1}{6}$ to $1\delta_y$) each step with three cycles. As predicted, practically linear force-displacement relationship and elastic buckling of the infill plates were observed during several early displacement steps. However, at the end of displacement Step 4 (= 0.36%), when the specimen reached the expected effective yield displacement of 12.4 mm, noticeable signs of yielding were observed. These were indicated by permanent buckling of the infill plate and residual displacement of approximately 3.1 mm. In addition, when the specimen pushed to the West at 0.36% drift, the maximum base shear obtained was 47 kN lower than that recorded when the specimen pulled to the East (i.e., 324 kN versus 371 kN). It was speculated that the belt used to connect West and East columns might contribute to this discrepancy by providing some degree of resistances to the specimen within the pulling stage.

During displacement Step 5, at 24.8 mm target displacement (= 0.72% drift = $2\delta_y$), uplifts and slips of approximately 4.7 mm and 3.7 mm, respectively, were observed at the clevis bases. Hence, all bolts were tightened, and smaller jacking actuators were installed along the direction of loading to prevent slips at the base. With these adjustments, the experimental program resumed with three cycles at 37.3 mm target displacement (= 1.09% drift = $3\delta_y$). The permanent buckling of the infill plate was more pronounced in this displacement Step 6 than in the previous steps. Uplifts and slips were closely monitored, and a slight increase of less than 2 mm was recorded. Furthermore, an out of plane movements of approximately 13.7 mm was recorded when the specimen reached its target displacement in Step 6. This indicated that the lateral supports provided were not capable to prevent the movement completely.



The experimental program continued to a higher displacement target of 49.7 mm ($= 1.45\%$ drift $= 4\delta_y$) for 2 cycles. During the first cycle of this displacement Step 7, flange local buckling and yielding of shear tabs (Fig. 4a) were observed at the WUF-W connections. At the end of the second cycle, however, fracture was observed at the West connection of the bottom beam (Fig. 4b). While flaking of whitewash was noted on the infill plate, no plate tearing was observed up to this point. The resulting peak base shears when cycling at 1.45% drift amplitude were 527 and 749 kN for the pushing (West) and pulling (East) excursions, respectively. Yielding around the shear tabs and flaking of whitewash on the infill plate spread to a larger area when the specimen was pushed to a higher displacement target of 85.8 ($= 2.5\%$ drift $= 6.9\delta_y$) in Step 8. In addition, flange local buckling increased (Fig. 5a) and fractures of moment connections were observed at continuity plates on panel zones (Fig. 5b) and at shear tabs (Fig. 5c) The hysteretic curve showed minor strength degradation when pushed in the West direction with recorded base shear of 498 kN. For the East excursion, however, the recorded base shear was 772 kN, slightly increased from that in the previous step.

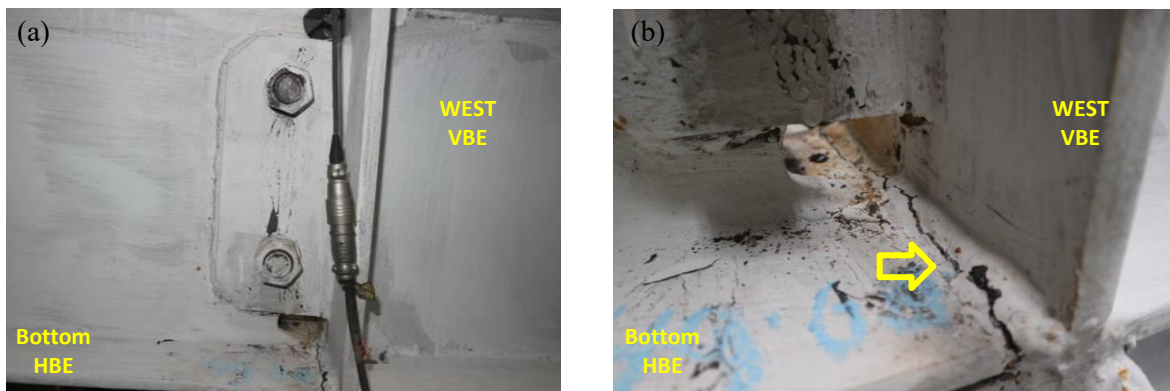


Fig. 4 – Specimen Condition During Step 7 (1.45% drift $= 4\delta_y$): (a) Shear Tab Yielding; (b) Weld fractures

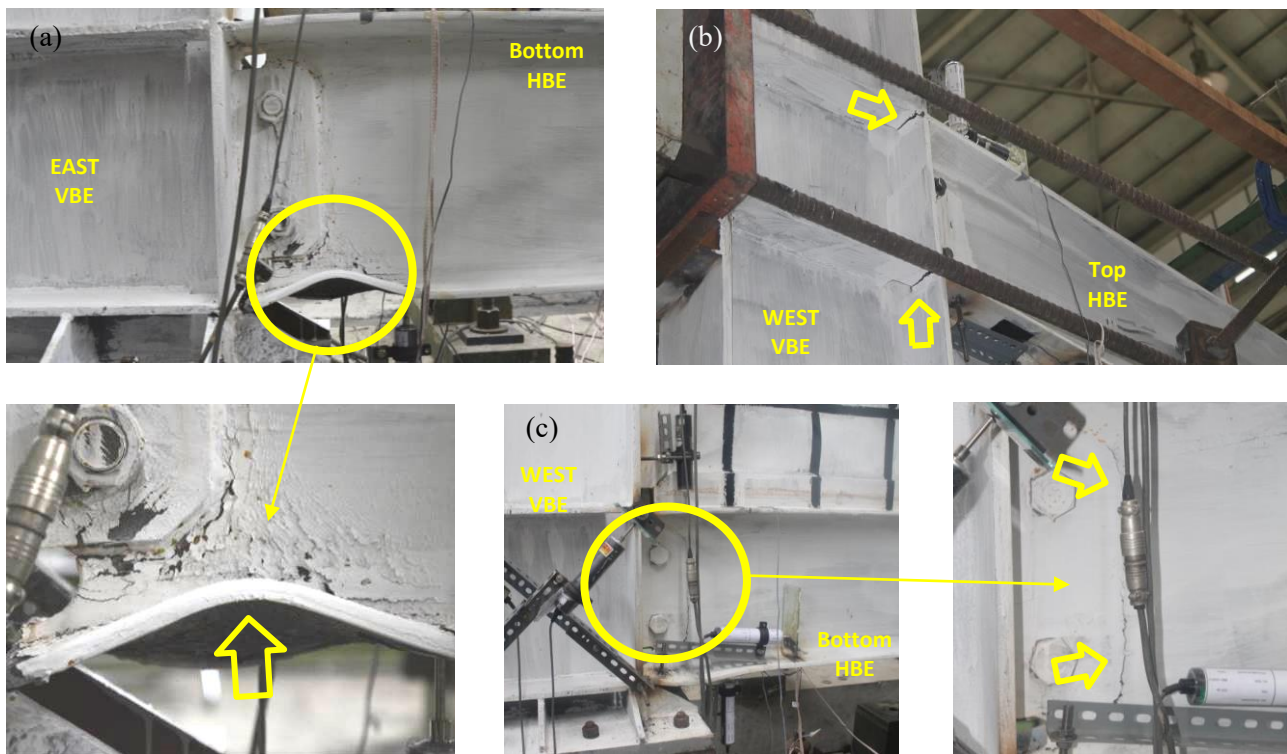


Fig. 5 – Specimen Condition During Step 8 (2.5% drift $= 6.9\delta_y$): (a) Flange Local Buckling; (b) Fractures of Continuity Plate; (c) Fractures of Shear Tabs



After half-way through the first cycle of the displacement Step 9 at 102.9 mm displacement target ($= 3.0\%$ drift $= 8.29\delta_y$), the test was stopped because lateral supports were inadequate any longer to prevent the specimen to move out-of-plane. The specimen experienced a 47 mm out-of-plane movement when the target displacement reached. Fig. 6(a) presents a complete hysteretic curve recorded for the WUF-W specimen, plotting the base shear versus top story displacement. Incidentally, the amount of slips occurred at the base have deducted from the top story displacement. The hysteretic curve exhibits a typical pinching behavior reported in past experimental research (e.g., [5, 7, 18]), stable and ductile behavior when undergoing large lateral drifts, and relatively small strength degradation between cycles at the same displacement step. Final condition of the WUF-W specimen is shown in Figs. 7 and 8. Large flange local buckling, significant plastification, or fractures were observed at the WUF-W connections.

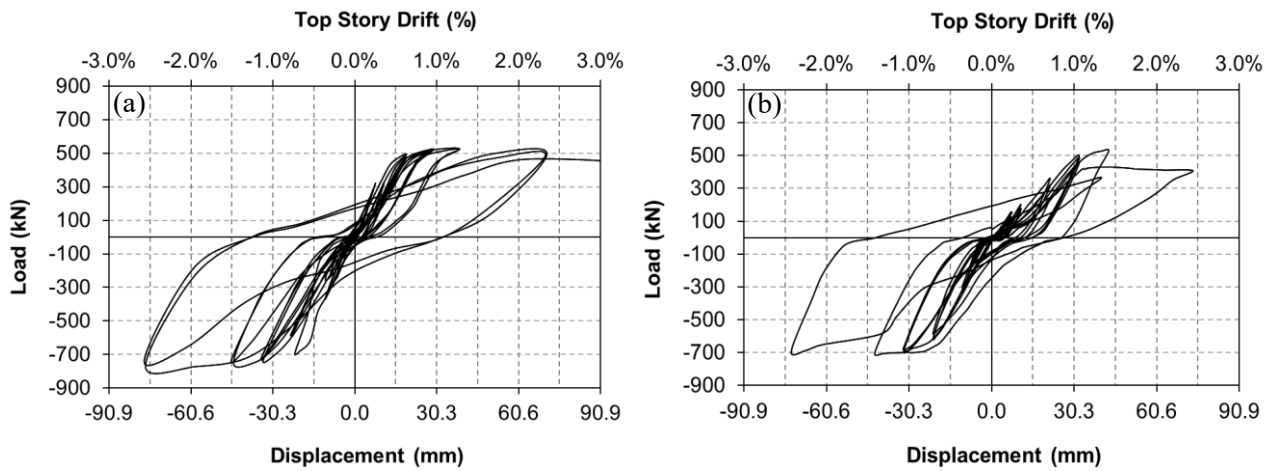


Fig. 6 – Base Shear versus Interstory Displacement: (a) WUF-W Specimen; (b) RBS Specimen



Fig. 7 – Final Condition of WUF-W Specimen at the Bottom HBE-to-VBE Connections: (a) East Connection, South View; (b) Detail of (a); (c) West Connection, South View; (d) Detail of (c)



Fig. 8 – Final Condition of WUF-W Specimen at the Top HBE-to-VBE Connections: (a) East Connection, South View; (b) and (c) Detail of (a); (d) West Connection, North View; (e) Detail of (d)

4.2 RBS Specimen

Testing of RBS specimen began with three cycles at a target displacement of 2.0 mm ($= 0.06\%$ drift $= \frac{1}{6}\delta_y$) in Step 1 and gradually increased to 24.0 mm ($= 0.71\%$ drift $= 2\delta_y$) in Step 5. Overall, specimen behavior was similar to that previously observed in the WUF-W specimen. Here, infill plates buckled elastically during several early displacement steps followed by buckled permanently at larger displacement steps. The maximum base shear recorded during the West and East excursion was somewhat different (i.e., 359 kN versus 617 kN when the specimen pushed and pulled, respectively, at 0.71% drift). In addition, signs of yielding were observed at RBS locations.

During displacement Step 6, at 36.0 mm target displacement ($= 1.06\%$ drift $= 3\delta_y$), out of plane movements of 22.4 and 11.6 mm were recorded at the top of West and East column, respectively. This twisting of columns increased to 51.0 and 53.2 mm at the respective locations, when the specimen was cycled at 48.0 mm target displacement ($= 1.41\%$ drift $= 4\delta_y$) in displacement Step 7. As a consequence of this significant out of plane movements, testing was performed only once cycle in this step. Several LVDTs were removed to prevent unexpected damage to them. However, no major damage was occurred on the infill plate, other than minor cracks at its corners. Yielding at the RBS locations and panel zones spread to a larger area. In addition, the resulting peak base shears when cycling at 1.41% drift amplitude were 527 and 705 kN for the West and East excursions, respectively.

After tightened all bolts at the lateral supports and while closely monitoring it, the experimental program then continued one more cycle to a higher displacement target of 85 mm ($= 2.5\%$ drift) in displacement Step 8, with an expectation whether new events such as damages at RBS locations would have been observed. However, no damage was occurred at RBS locations, other than significant plastification at the cutouts and panel zone locations (Fig. 9). Due to twisting of columns, as shown in Fig. 10, testing was concluded to prevent damage to the lateral supports that may have occurred. Fig. 6(b) presents a complete



hysteretic curve recorded for the RBS specimen. Incidentally, due to some instrumentation issues, displacement records of the last cycle were inferred from three LVDTs that measured specimen lateral displacements at the top beam level.

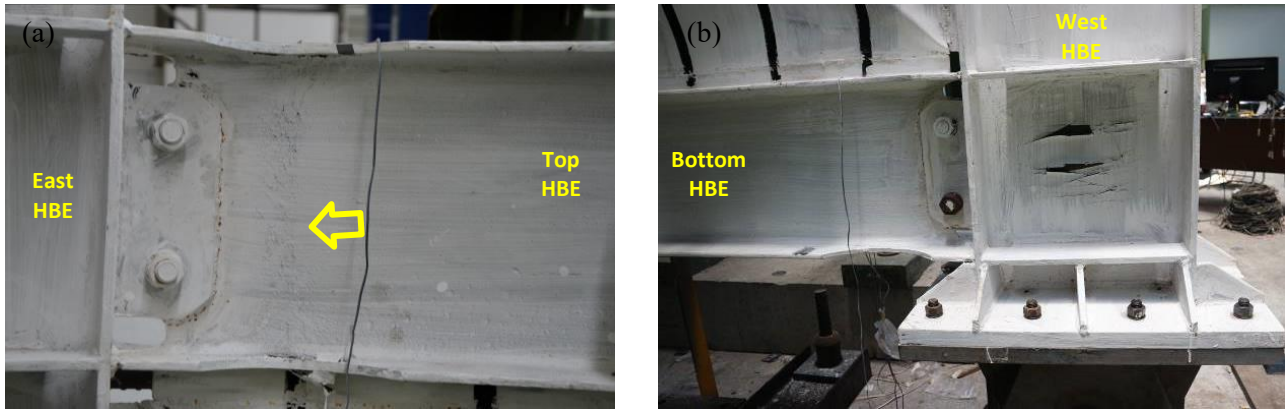


Fig. 9 – Signs of Plastification of RBS Specimen Step 8 (2.5% drift): (a) at Cutouts; (b) at Panel Zone

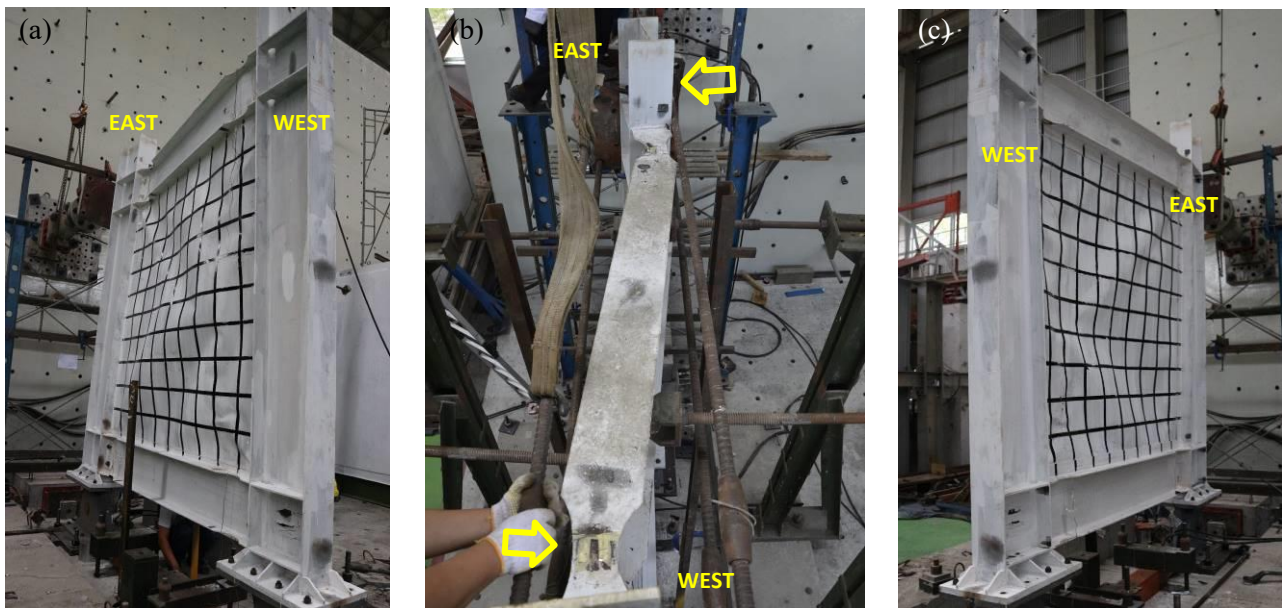


Fig. 10 – Final Condition of RBS Specimen: (a) North View; (b) Top View Showing Twisting of Columns; (c) South View

5. Conclusions

Two large-scale experimental programs were designed and tested to investigate the behavior of special moment resisting connections (SMRC) in SPSWs. The performance of eight WUF-W and RBS type connections (two of the prequalified connections specified in the AISC 358-16 documents) were observed. After pushover cyclic tests with target drifts at the top beam gradually increased from 0.06% to 3.0% drift, large flange local buckling, significant plastification, or fractures occurred at all SMRC connections. This research also provided an additional evidence that ordinary-type connections used in SPSWs might not be sufficient to sustain large rotation demand that could develop in those HBE-to-VBE connections. Future research is needed to assess the performance of other prequalified special moment resisting connections.



6. Acknowledgements

This work was supported by the Directorate Research and Community Services, Directorate General of Research Strengthening and Development of the Indonesian Ministry of Research, Technology, and Higher Education under Postdoctoral Research Grants No. 165/LPPM/IV/2017 and No. 2231/SP2H/LT/K2/KM/2018. However, any opinions, findings, conclusions, and recommendations presented in this paper are those of the writers and do not necessarily reflect the views of the sponsors. The assistance of Ruri Damayanti, Sella Gita Rizkia, and Didi Prasetyo during the experimental programs and manuscript preparation is also appreciated.

7. References

- [1] Sabelli R, Bruneau M (2007): Steel plate shear walls. *AISC Design Guide*. Chicago, Illinois. American Institute of Steel Construction, Inc.
- [2] Bruneau M, Uang CM, Sabelli R (2011): *Ductile design of steel structures*. 2nd edition. New York, McGraw-Hill.
- [3] AISC (2010): Seismic provisions for structural steel buildings. ANSI/AISC 341-10. American Institute of Steel Construction, Inc., Chicago, Illinois.
- [4] CSA (2009): Design of steel structures. CAN/CSA S16-09. Canadian Standards Association, Willowdale, Ontario, Canada.
- [5] Driver RG, Kulak GL, Kennedy DJL, Elwi AE (1997): Seismic behavior of steel plate shear walls. *Structural Engineering Report 215*. Department of Civil Engineering, University of Alberta, Edmonton, Alberta, Canada.
- [6] Lubell AS, Prion HG, Ventura CE, Rezai M (2000): Unstiffened steel plate shear wall performance under cyclic loading. *Journal of Structural Engineering*, **126** (4), 453-459.
- [7] Vian D, Bruneau M, Tsai KC, Lin Y-C (2009): Special perforated steel plate shear walls with reduced beam section anchor beams. I: experimental investigation. *Journal of Structural Engineering*, **135** (3), 211-220.
- [8] Park HG, Kwack JH, Jeon SW, Kim WK, Choi IR (2007): Framed steel plate wall behavior under cyclic lateral loading. *Journal of Structural Engineering*, **133** (3), 378-388.
- [9] Qu B, Bruneau M, Lin CH, Tsai KC (2008): Testing of full-scale two-story steel plate shear wall with reduced beam section connections and composite floors. *Journal of Structural Engineering*, **134** (3), 364-373.
- [10] Purba R, Bruneau M (2014): Seismic performance of steel plate shear walls considering two different design philosophies of infill plates. I: deterioration model development. *Journal of Structural Engineering*, 1-12.
- [11] Purba R, Bruneau M (2015): Experimental investigation of steel plate shear walls with in-span plastification along horizontal boundary elements. *Engineering Structures*, **97**, 68-79.
- [12] AISC (2010): Prequalified connections for special and intermediate steel moment frames for seismic applications. ANSI/AISC 358-10. American Institute of Steel Construction, Inc., Chicago, Illinois.
- [13] AISC (2016): Prequalified connections for special and intermediate steel moment frames for seismic applications. ANSI/AISC 358-16. American Institute of Steel Construction, Inc., Chicago, Illinois.
- [14] Purba R, Bruneau M (2012): Case study on the impact of horizontal boundary elements design on seismic behavior of steel plate shear walls. *Journal of Structural Engineering*, **138** (5), 645-657.
- [15] AISC (2016): Seismic provisions for structural steel buildings. ANSI/AISC 341-16. American Institute of Steel Construction, Inc., Chicago, Illinois.
- [16] Berman JW, Bruneau M (2008): Capacity design of vertical boundary elements in steel plate shear walls. *Engineering Journal*, **45** (3), 57-71.
- [17] ATC-24 (1992): Guidelines for cyclic seismic testing of components of steel structures. Applied Technology Council, Redwood City, CA.
- [18] Choi IR, Park HG (2009): Steel plate shear walls with various infill plate designs. *Journal of Structural Engineering*, **135** (7), 785-796.